Application of an optimal control strategy for solar power plants operating in a day-ahead market scheme ⋆

Paulo H. F. Biazetto * **Gustavo A. de Andrade** *
Julio E. Normey-Rico *

* *Departamento de Automação e Sistemas, Universidade Federal de Santa Catarina, Florianópolis, Brazil (e-mail: paulo.biazetto@posgrad.ufsc.br, gustavo.artur@ufsc.br, julio.normey@ufsc.br)*

Abstract: Thermal solar power plants operating in a day-ahead market scheme aim to maximize the solar energy captured in the solar collector fields and the electric energy revenue in the power block according to the energy tariff. Classic control strategies are not able to obtain good performance for this kind of framework because of the variability of the energy tariff profile over the days. In this context, this work presents the assessment of the potential of an optimal controller to increase the profitability of the plants. Simulation results with energy tariffs and meteorological data from Spain are presented in order to illustrate the performance of the methodology. Finally, a comparative study with a classic control strategy shows the improvements in the energy revenue produced in this scenario.

Keywords: Energy production; Optimal control; Renewable energy; Thermal solar power plants; Thermal Energy Storage.

1. INTRODUCTION

Global energy and electricity consumption is increasing rapidly due to population growth, industrialization, and urbanization. In the last four decades, the world energy demand and carbon dioxide (CO_2) production have more than doubled and, according to the projections in Agency (2020) which incorporates existing energy policies as well as an assessment of the results likely to stem from the implementation of announced political intentions, an increase of 6.19% in the world production of CO_2 is expected until 2040. In a scenario of sustainable development with public policies that outlines an integrated approach to achieving internationally agreed objectives on climate change, air quality, and universal access to energy, it is expected that CO_2 emissions would reduce 52.86%. Researches have shown that solar, wind, and biomass energies are the most promising ones and they can contribute to increasing energy production and reducing environmental impacts caused by fossil fuels.

Solar thermal energy generation systems are composed of a solar collector field, a power cycle and a thermal energy storage (TES) system that allows the plant to operate at staggered times instead of only in the current solar energy dispatch mode. A comprehensive review of concentrating solar power (CSP) plants and some new concepts for the integration of TES systems into them can be found in Alva et al. (2018). From a control point of view, the control strategies for CSP systems aim at maintaining the solar collector outlet temperature close to its nominal value in spite of disturbances by varying the Heat Transfer Fluid (HTF) mass flow rate. In this context, many methodologies have been proposed in the literature. The approaches range from feedback linearization controllers (Cirre et al., 2007) to model-based predictive controllers (Andrade et al., 2013) or adaptive control (Lemos et al., 2014).

When a TES system is integrated into the CSP plant, an additional control variable – the mass flow rate from the storage tank to the power block – can be included in the control problem in order to exploit the dispatchability capacities of the overall system. Recently, an optimal control strategy was proposed in Biazetto et al. (2021) to maximizes the usage of the thermal energy captured by CSP plants. Using such a methodology, the levelized cost of energy (LCOE) of the plant may decrease even more.

In this paper, the methodology proposed in Biazetto et al. (2021) is applied in a solar power plant operating in a day-ahead price market scheme. In several countries, such framework is currently adopted, such as the USA, Spain, Belgium, Italy, and Germany (Casati et al., 2015), and it allows buyers and sellers to hedge against price volatility in the real-time energy market by locking in energy prices before the operating day. Notably, however, classic control strategies currently available in the literature, like those presented in Wagner and Gilman (2011), are not able to obtain a good cost per kW of solar power because of the variability of energy tariff profiles over the days. In this context, this work presents the assessment of the potential of the optimal controller in order to increase the profitability of the plants. The study performed in this paper is based on the Spain price market under a range

⋆ This work was partially supported by CNPq and Petrobras.

of scenarios with solar radiation and ambient temperature compared to a classic control strategy in order to highlight the benefits of the optimal control methodology in terms of revenue.

The rest of the paper is organized as follows: Section 2 presents a brief description of the plant, its operating modes and the formulation of the mathematical model. The control problem is described in Section 3. The proposed optimal control methodology is presented in Section 4, whereas a reference control strategy is given in Section 5. Simulation results and a comparative study between these control strategies are shown in Section 6. Finally, the concluding remarks are stated in Section 7.

2. PLANT DESCRIPTION

The CSP system considered in this work it is based on the Fresnel collector technology (see Figure 1) and uses molten salts as HTF. The main characteristics of this mixture are the high heat transfer coefficient, thermal stability, low cost and not be flammable. As can be seen in Figure 1, both TES systems are positioned in series with the solar collector fields, and thus, completely decouple the solar collector field from the power block.

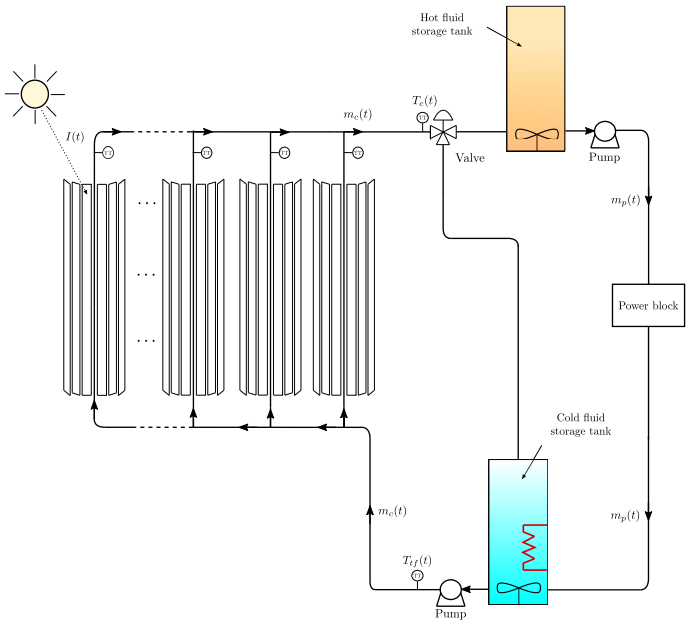

Figure 1. Schematic diagram of the CSP plant (Biazetto et al., 2021).

2.1 Operation Modes

The solar power plant considered in this work has several operating modes, which are defined by switching the valve located at the end of the solar field (see Figure 1):

- **Start-up:** The HTF recirculates between the cold TES system and the solar collector field through the pump. This operating mode only happens during the light phase of the day and lasts until the outlet temperature of the solar collector field reaches a minimum outlet temperature value, $T_{c,rec}$.
- **Nominal:** The outlet temperature of the solar collector field is set to its nominal reference temperature, $T_{c,ref}$. The HTF moves from the solar collector field to the hot TES system, which will then feed a heat exchanger in the power block in order to generate steam for a turbine. After being used in the heat exchanger, the HTF returns to the cold TES and is pumped to the solar collector field to restart the cycle.
- **Shut-down:** During this mode, the hot TES system stops receiving fluid from the solar field. The solar collector field operates recirculating the HTF in the cold TES system. The warm fluid dispatch continues until the hot tank runs out.
- **Night and anti-freeze:** This operation mode aims to keep the temperature limits within an acceptable and safe range, mainly conditioning the fluidity of the HTF in the pipes. An electrical resistance inside the cold TES system is used to induce heat to the plant.

2.2 Mathematical Model

In this section, the main equations of the CSP plant will be briefly presented since they are standard in the literature (Biazetto et al., 2021; Camacho et al., 2012).

Heat Transfer Fluid The thermodynamic properties of the molten salts can be described by the following equations (Lopes et al., 2020):

$$h(T) = 1435.5\,T + 422740, \tag{1}$$
$$\rho(T) = 2240 - 0.8266\,T, \tag{2}$$
$$c_p(T) = 1546.2 - 0.3\,T, \tag{3}$$

where h is the specific enthalpy [J/kg], ρ is the specific mass [kg/m^3], c_p is the specific heat [J/kg $^{\text{o}}$C] and T is the temperature [$^{\text{o}}$C].

In the next sections, the notation h_i, ρ_i and $c_{p,i}$ is used to represent the thermodynamic property of the HTF in the subsystem i calculated from its temperature, T_i.

Solar Collector Field The outlet temperature of the solar collector field is given by the following equation (Camacho et al., 2012):

$$\rho_c\, c_{p,c}\, A_c\, \frac{dT_c}{dt} = \alpha\, \gamma\, G\, I - \frac{c_{p,c}\, m_c\, (T_c - T_{tf})}{\eta_{op}\, L} - \frac{\tilde{H}_l\,(T_m,\, T_{amb})}{L_2}, \tag{4}$$

where (arguments have been omitted for readability) t is the time and belongs to $[0, \infty)$, T_c (controlled variable) is the outlet temperature [$^{\text{o}}$C], T_{tf} is the inlet temperature [$^{\text{o}}$C] – which is given by the outlet temperature of the cold TES system (see Figure 1) –, T_m is the average between T_c and T_{tf}, and T_{amb} is the ambient temperature [$^{\text{o}}$C]. The outlet mass flow rate [kg/s] is given by $m_c \in [m_c^{min},\, m_c^{max}]$ (control variable), with $0 < m_c^{min} < m_c^{max}$, while the specific mass [kg/m^3] and specific heat [J/(kg $^{\text{o}}$C)], both computed from T_c, are given by ρ_c and $c_{p,c}$, respectively. The solar radiation [W/m^2] is given by I, the collector optical efficiency is given by $\alpha \in [0,\, \alpha^{max}]$, where $\alpha^{max} \in (0,\, 1]$, its aperture [m] is given by G and $\gamma \in [0,\, 1]$ represents the defocus of the collectors (control variable). The pipe cross-section area [m^2] is denoted by A_c, the length of the loop [m] is given by L, the number of loops is

η_{op} and L_2 denotes the total length of the solar collector field [m]. The term $\tilde{H}_l$ [J/s] represents the thermal losses by convection. Finally, the initial condition of (4) is $T_c(0) = T_c^0$, with $T_c^0 \in \mathbb{R}$.

Thermal Energy Storage The storage tanks are of the vertical cylindrical type with a flat bottom. It is assumed that these tanks are operating at ambient pressure and the same temperature throughout the volume, that is, perfect mixture. Thus, the following mass balances are satisfied Egeland and Gravdahl (2002):

$$A_{tq}\,\rho_{tq}\,\frac{dL_{tq}}{dt} = m_c\,\beta - m_p, \tag{5}$$

$$A_{tf}\,\rho_{tf}\,\frac{dL_{tf}}{dt} = m_p - m_c\,\beta, \tag{6}$$

where the sub-indices tq and tf represent the variables of the hot and cold TES systems, respectively. For $i \in \{tq, tf\}$, L_i is the HTF level [m] of the tank i and A_i represents its cross-sectional area [m^2]. The outlet mass flow rate [kg/s] of the hot TES system is denoted by $m_p \in [0, m_p^{max}]$ (control variable), with $m_p^{max} > 0$, at the same time m_p is the mass flow rate from the power block to the cold fluid TES system. It is important to emphasize that the power block dynamics were neglected in this work. In this way, it is assumed that the power block outlet temperature is assumed to be constant and equal to its nominal operating value. The outlet mass flow rate [kg/s] of the cold TES system is given by m_c. β represents a Boolean function which imposes the plant's operating mode according to the description in Section 2.1.

The initial condition of (5)-(6) is $L_{tq}(0) = 0$ and $L_{tf}(0) = L_{tf}^0$, respectively, with $L_{tf}^0 \in \mathbb{R}_+$.

The HTF temperature behavior in the hot and cold TES systems are captured by the following equations, respectively:

$$L_{tq}\,A_{tq}\left(h_{tq}\frac{d\rho_{tq}}{dT_{tq}} + \rho_{tq}\frac{dh_{tq}}{dT_{tq}}\right)\frac{dT_{tq}}{dt} = m_c\,\beta\,(h_c - h_{tq}) - \tilde{P}_l\,(T_{tq} - T_{amb}), \tag{7}$$

$$L_{tf}\,A_{tf}\left(h_{tf}\frac{d\rho_{tf}}{dT_{tf}} + \rho_{tf}\frac{dh_{tf}}{dT_{tf}}\right)\frac{dT_{tf}}{dt} = m_c\,(1-\beta)\,(h_c - h_{tf}) + m_p\,(h_p - h_{tf}) - \tilde{P}_l\,(T_{tf} - T_{amb}) + Q, \tag{8}$$

for $i \in \{tq, tf\}$, T_i is the temperature [ºC] of the fluid in the tank i, being T_{tf} a controlled variable, and $Q \in [0, Q^{max}]$, with Q^{max}, represents the heat [W] released by the electrical resistance (control variable) in the cold TES system. The specific enthalpy [J/kg] of output from the solar collector field is given by h_c and the specific enthalpy [J/kg] of output from the power block is given by h_p. The term $\tilde{P}_l$ [kJ/s] is the coefficient of thermal losses of the tanks by convection and it is assumed to be a positive constant.

The initial condition of (7)-(8) is $T_{tq}(0) = T_{tq}^0$ and $T_{tf}(0) = T_{tf}^0$, respectively, with $T_{tq}^0, T_{tf}^0 \in \mathbb{R}$.

3. CONTROL PROBLEM

As already described in Section 2, the series configuration TES system completely decouples the solar collector field from the power block, allowing thus to translate the CSP plants control problem into two subproblems.

The first one is related to the solar collector field. The controller objective in this subsystem is to maintain the outlet temperature in the desired reference value. To achieve this goal, the HTF mass flow rate through the solar field is considered a control variable. Importantly, the controller must also defocus the mirrors to prevent that the thermal power induced by solar radiation degrades the HTF.

The second control subproblem is related to the TES system and the storage/dispatch of the HTF for the power block, and it aims to maximize the daily revenue from the electricity sale. In this context, the controller must compute the outlet mass flow rate of the hot TES system. The control system must avoid the power block operation below a minimum load and fast changes of the mass flow rate, as well as repeated re-starts of the power block during the same day to ensure a feasible operation. It also must ensure that the HTF in the cold TES system remains around the desired temperature reference by manipulating the electrical resistance located in the cold TES system in order to prevent its freezing during the night.

4. OPTIMAL CONTROL

This section presents the optimal control methodology studied in this paper. Such strategy was first proposed in Biazetto et al. (2021), and thus, only the main steps will be described in the following.

4.1 Solar Collector Field

Let $U_0 = (\gamma,\ m_c,\ \beta)$ be the vector of control variables and consider the following time interval $t \in [0, t_f]$, with t_f a fixed value. Then, the following continuous time optimization problem is obtained:

$$\begin{aligned} P_0:\ \min_{U_0(t)\,\in\,\mathcal{U}_0} & \int_0^{t_f} \Big(c_0\,(T_{c,ref} - T_c)^2 + c_1\,m_c^2 \\ & \qquad -\alpha\,\gamma\,G\,I + \beta\,(T_{c,rec} - T_c)\Big)dt, \\ \text{s. t.:}\ & \text{Equation (4)}, \\ & T_c(0) = T_c^0, \end{aligned} \tag{9}$$

in which

$$\mathcal{U}_0 = \{(\gamma,\, m_c,\, \beta) \in \mathbb{R}^3 \mid\ 0 \le \alpha\,\gamma\,G\,I \le \alpha_{max}\,G\,I_{max},\ m_{c,min} \le m_c \le m_{c,max},\ 0 \le \beta \le 1\}.$$

In (9), the term $T_{c,ref} \in \mathbb{R}$ denotes the outlet reference temperature [ºC] of the solar collector field in nominal operating mode, $T_{c,rec} \in \mathbb{R}$ is the temperature value to switch between the start-up and nominal operating modes, and $c_0 > 0$ and $c_1 \ge 0$ are control design parameters.

4.2 Thermal Energy Storage

The constraints involved in the repeated re-starts in the power block, its minimum load allowed and the prevention

of fast changes in the mass flow rate at the outlet of the hot TES system are technically challenging in the optimal control formulation because of the time derivative of the control variable in the cost function. To tackle this issue, m_p will be decomposed into two new variables, i.e., $m_p = m_p^c + m_p^d$, with m_p^c absolute continuous and m_p^d a step function, such that $m_p^d \leq 0$. Then, $\frac{dm_p}{dt} = \frac{dm_p^c}{dt}$ and defining $r = \frac{dm_p}{dt}$, it follows that $\frac{dm_p^c}{dt} = r$, i. e., r determines the absolute continuous part of m_p. In other words, the problem of finding m_p is rewritten as the problem of finding r and m_p^d.

Then, defining $U_1 = (r,\, m_p^d,\, Q)$, the following optimization problem is formulated for the time interval $t \in [0, t_f]$:

$$
\begin{aligned}
P_1: \quad & \min_{U_1(t)\,\in\,\mathcal{U}_1} \int_0^{t_f} \Big(-\eta\,(m_p^c + m_p^d)\,P_w \\
& \qquad + c_2\,(T_{tf,ref} - T_{tf})^2 + c_3\,m_p^d\,(f_{min} - m_p^c) \\
& \qquad\qquad + c_4\,r^2 + c_5\,Q^2 \Big) dt, \\
\text{s. t.:} \quad & \text{Equations } (5)-(8), \\
& \frac{dm_p^c}{dt} = r, \\
& 0 \leq L_{tq} \leq L_{tq,max}, \\
& 0 \leq L_{tf} \leq L_{tf,max}, \\
& T_{tq}(0) = T_{tq}^0, \quad T_{tf}(0) = T_{tf}^0, \\
& L_{tq}(0) = 0, \quad\;\; L_{tf}(0) = L_{tf}^0, \\
& m_p^c(0) = 0,
\end{aligned}
\tag{10}
$$

with

$$
\mathcal{U}_1 = \{(r,\, m_p^d,\, Q) \in \mathbb{R}^3 \mid\; 0 \leq Q \leq Q_{max},\; m_p^d \leq 0,\; 0 \leq m_p^c + m_p^d \leq m_p^{max}\}.
$$

In (10), the efficiency of the power block is given by η, while c_2, $c_3 > 0$ and c_4, $c_5 \geq 0$. Note that the first term of the functional in (10) is responsible for the instant revenue from the sale of electricity. The price of the electricity produced is given by $P_w = TOD \cdot PPA$, in which TOD is the time of day and PPA (*Power Purchase Agreement*) represents the energy purchase [Price/kW]. The second term of the functional in (10) has been included to keep the fluid temperature in the cold storage tank at the desired reference value $T_{tf,ref}$. In turn, the third term prevents the power block from working below the minimum operating mass flow rate, f_{min}, with $f_{min} \in (0,\, m_p^{max})$. The minimum load for dispatch is defined as a restriction so that the thermal energy storage system only dispatches to the power block above the desired value. This condition prevents the power block from operating in low conditions, disturbing as little as possible the optimization of the first term, i.e., the economic revenue of the plant. The fourth term was introduced to penalize rapid changes in r. The fifth term of the functional in (10) penalizes rapid changes in the heat induced by the electrical resistance in the cold fluid storage tank. Finally, the last two inequalities in (10) were included to restrict the liquid levels in the storage tanks within the feasible range of operation.

5. CLASSIC CONTROL STRATEGY

The optimal control strategy, described in the previous section, will be compared to a classic control strategy that aims at satisfying the nominal power cycle demand by making use of the available resources in the TES system while ensuring that the operative constraints are satisfied. The methodology considers a PI controller with an anti-windup strategy for the regulation of the outlet temperature of the solar collector field, where the design parameters were obtained based on the AMIGO tuning rule. A feedforward controller is also considered for defocusing the solar field when it exceeds the nominal thermal power of the plant.

This classic control strategy uses a priority dispatch list, which contains the time instant of the day where the HTF in the hot TES system must be dispatched to the power block on each day. The computation of these time instants is performed as follows. First, the solar collector field subsystem is simulated decoupled from the TES system [1] in order to define its outlet mass flow rate and temperature behavior during the day. These data are then used in the hot TES subsystem equations to predict its behavior. With a sampling time of 30 minutes, the switching time of m_p from its minimum value to maximum value (and vice versa) is determined within the TES physical constraints. Obviously, days with a high solar radiation profile will induce high mass flow rates in the solar collector field, and consequently, the algorithm should prioritize the saturation limits of the thermal energy in the TES over the energy tariff prices. For days with a low solar radiation profile, thermal energy saturation is not expected and the dispatch can give priority to the maximum energy tariff price periods.

6. SIMULATION RESULTS

The numerical tests were conducted considering (4)-(8) as a virtual plant and real weather data from Spain corresponding to the geographic location 37º05'27.8"N 2º21'19.0"W over six days were considered. The energy tariff profile for this scenario comes from the day-ahead price in the stock market, which is available in OMIE (2021).

The simulations were coded in MATLAB and the CasADi package (Andersson et al., 2019) was used to solve the optimal control problem numerically. To ensure proper numerical conditioning of the solver, the system variables were made dimensionless in order to get a system with normalized variables of similar sizes. A design parameter called the solar multiple (SM) normalizes the size of the solar field concerning the power block in nominal operation (Jorgenson et al., 2013). Therefore, a larger SM implies a larger solar collector area. Importantly, the plant's SM has a value of 2.3 approximately, and the TES system has a storage capacity of 4 hours. The power block efficiency is $\eta = 60\%$ and the (dimensionless) minimum operating mass flow rate of the power block is $f_{min} = 0.72$. The sampling time and the prediction horizon are defined as 6 minutes and 15 hours, respectively. Tests with a sampling time of 1 minute show similar results, however, they require a higher computational cost. An interpolation of the solar radiation, ambient temperature, and optical efficiency data

[1] This situation is reasonable since the temperature of the cold TES system is approximately constant and there is always enough HTF to be directed to the solar field under normal operating conditions.

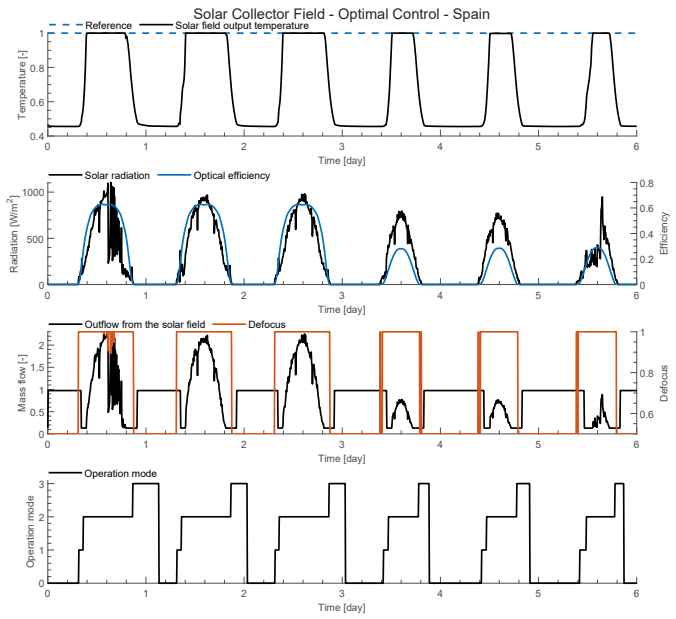

Figure 2. Simulation results of the plant with the Optimal Control Strategy.

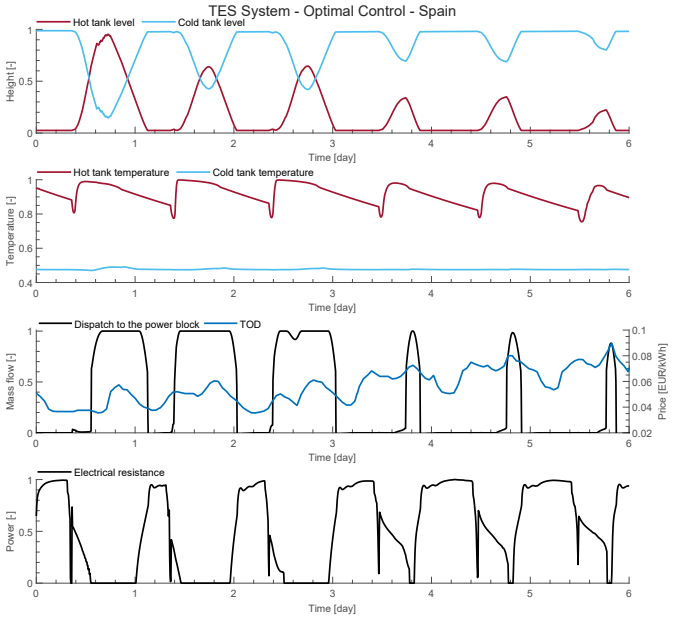

Figure 3. Simulation results of the plant with the Optimal Control Strategy.

is performed to approximate the values to the desired sampling time time. In the case of Classic Control Strategy, the sample time is 30 seconds. For readability reasons, the operation modes described in Section 2.1 will be labeled as follows: 0 - night; 1 - start-up; 2 - nominal; and 3 - shut-down.

6.1 Optimal Control

Figure 2 shows the time evolution of the main variables of the solar collector field with the Optimal Control Strategy. As can be seen in the first graphic of Figure 2, the optimal controller was able to track the outlet temperature reference during the day.

The time evolution of the variables associated with the TES system are presented in Figure 3. The level and temperature of the hot and cold TES are shown in the first and second graphics of Figure 3. Both tanks stay within the designed operating range, without saturating the levels. Additionally, the electrical resistance is only used during the night for the first three days. However, for the days of low radiation profile, the electrical resistance remains active for almost the whole day to keep the temperature of the cold TES system in the reference range. The optimal controller always dispatch the fluid in the hot TES system to the power block during the time interval with better tariff prices (see the third graphic of Figure 3). Finally, the minimum load to the power block is always satisfied at the same time that it does not present repeated restarts during the same day.

6.2 Classic Control Strategy

Figure 4 presents the time evolution of the main variables of the solar collector field with the Classic Control Strategy. As can be seen in the first graphic of Figure 4, the controller was able to track the outlet temperature reference during the day.

Figure 5 presents the time evolution of the variables associated with the TES system. As can be seen in the third graphic of Figure 5, the controller always tries to dispatch the HTF in the hot TES system during the time intervals with better energy tariff prices. However, there are some cases where the dispatch is not computed precisely. As there is a high variation in prices during the day, it is difficult to include such information in this strategy. Finally, the temperature of the cold TES system is maintained around its operating point by manipulating the electrical resistance (see the bottom graphic of Figure 5).

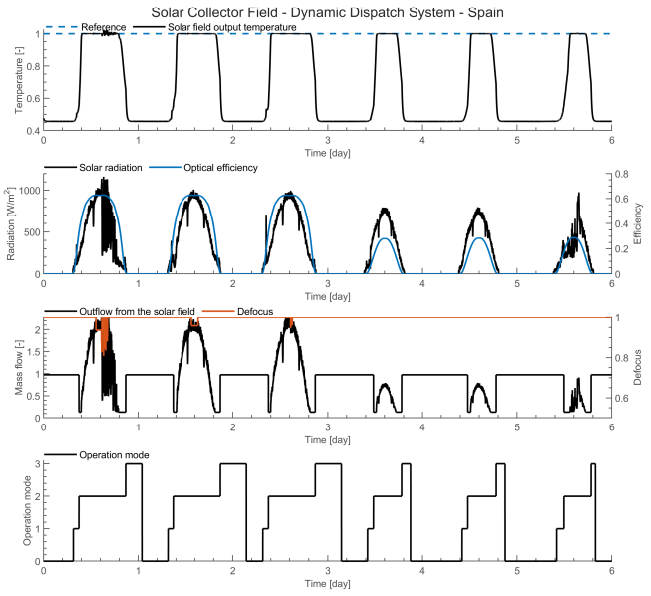

Figure 4. Simulation results of the plant with the Classic Control Strategy.

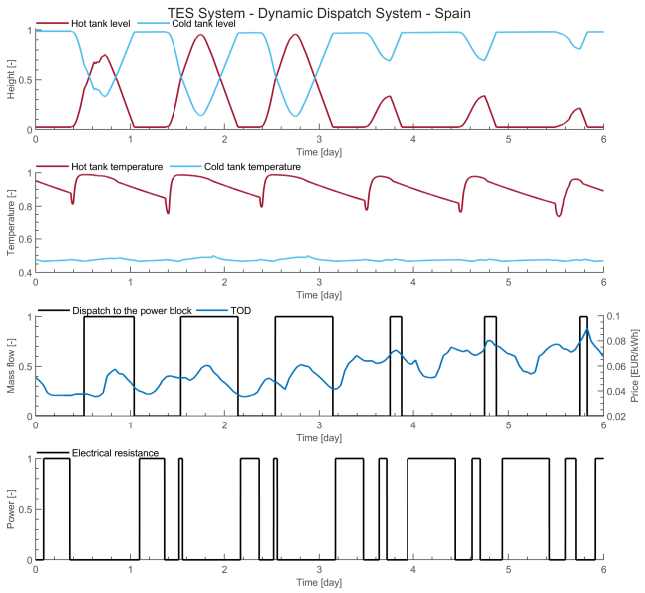

Figure 5. Simulation results of the plant with the Classic Control Strategy.

6.3 Discussions

The revenue gain of the plant for six days of operation with the optimal strategy in the Spanish energy tariff scenario was 5.45% over the classic controller, as can be seen in Figure 6. However, it is important to emphasize that this result considers an ideal scenario of the control problem, where knowledge of future solar radiation and perfect matching of the model and plant dynamics was assumed. This result may seem slightly optimistic, but it will represent the plant operation in a much more credible and perennial way than others obtained with simplified control policies.

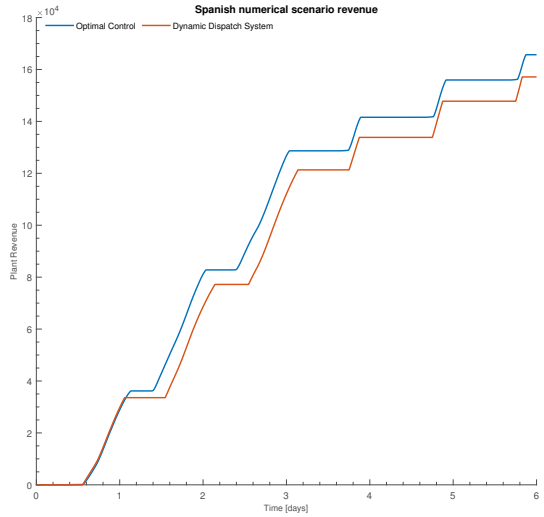

Figure 6. Plant revenue as a function of time for the Spanish numerical scenario.

7. CONCLUSION

This work studies the application of an optimal control strategy to a CSP system operating in the context of a time-varying tariff and day-ahead price market scheme. Simulation results showed that this methodology achieved higher revenue than a classic strategy currently used in real-life plants. Notably, however, the study was only performed for a specific condition of solar multiple and the results may vary depending on the conditions of storage capacity and size of the solar field.

REFERENCES

Agency, I.E. (2020). *Key World Energy Statistics 2020*. International Energy Agency. URL `https://www.iea.org/reports/key-world-energy-statistics-2020`.

Alva, G., Lin, Y., and Fang, G. (2018). An overview of thermal energy storage systems. *Energy*, 144, 341–378.

Andersson, J.A., Gillis, J., Horn, G., Rawlings, J.B., and Diehl, M. (2019). Casadi: a software framework for nonlinear optimization and optimal control. *Mathematical Programming Computation*, 11(1), 1–36.

Andrade, G., Pagano, D., Alvarez, J.D., and Berenguel, M. (2013). A practical nmpc with robustness of stability applied to distributed solar power plants. *Solar Energy*, 92, 106–122.

Biazetto, P.H.F., de Andrade, G.A., and Normey-Rico, J.E. (2021). Development of an optimal control strategy for temperature regulation and thermal storage operation of a solar power plat based on Fresnel collectors. *IEEE Transactions on Control Systems Technology (Submitted)*.

Camacho, E., Berenguel, M., Rubio, F.R., and Martínez, D. (2012). *Control of solar energy systems*. Springer-Verlag, London.

Casati, E., Casella, F., and Colonna, P. (2015). Design of csp plants with optimally operated thermal storage. *Solar Energy*, 116, 371–387.

Cirre, C.M., Berenguel, M., Valenzuela, L., and Camacho, E.F. (2007). Feedback linearization control for a distributed solar collector field. *Control Engineering Practice*, 15(12), 1533–1544.

Egeland, O. and Gravdahl, J.T. (2002). *Modeling and simulation for automatic control*, volume 76. Marine Cybernetics Trondheim, Norway.

Jorgenson, J., Denholm, P., Mehos, M., and Turchi, C. (2013). Estimating the performance and economic value of multiple concentrating solar power technologies in a production cost model. Technical report, National Renewable Energy Lab.(NREL), Golden, CO (United States).

Lemos, J.M., Neves-Silva, R., and Igreja, J.M. (2014). *Adaptive control of solar energy collector systems*, volume 253. Springer.

Lopes, T., Fasquelle, T., Silva, H.G., and Schmitz, K. (2020). Hps2-demonstration of molten-salt in parabolic trough plants-simulation results from system advisor model. In *AIP Conference Proceedings*, volume 2303. AIP Publishing LLC.

OMIE (2021). Day-ahead market hourly prices in spain. URL `"https://www.omie.es/en/file-access-list"`.

Wagner, M. and Gilman, P. (2011). Technical manual for the SAM physical trough model. Technical report, National Renewable Energy Laboratory.